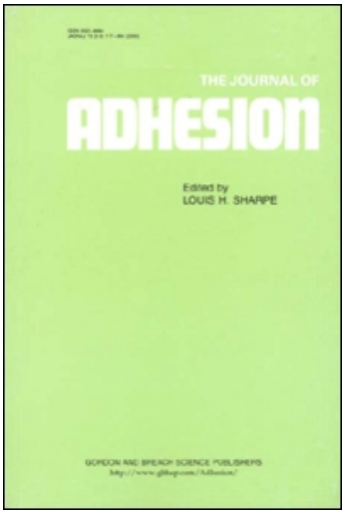

The Journal of Adhesion
Publication details, including instructions for authors and subscription information:
http://www.informaworld.com/smpp/title~content=t713453635

Characterisation of Amyloid Nanostructures in the Natural Adhesive of Unicellular Subaerial Algae

Anika S. Mostaert[ab]; Cristiano Giordani[b]; Rowena Crockett[c]; Ulf Karsten[d]; Rhena Schumann[d]; Suzanne P. Jarvis[b]
[a] School of Biology and Environmental Science, University College Dublin, Belfield, Dublin, Ireland [b] Conway Institute of Biomolecular and Biomedical Research, University College Dublin, Belfield, Dublin, Ireland [c] Swiss Federal Laboratories for Material Testing and Research, Duebendorf, Switzerland [d] Institute of Biological Sciences, Applied Ecology, University of Rostock, Rostock, Germany

To cite this Article Mostaert, Anika S. , Giordani, Cristiano , Crockett, Rowena , Karsten, Ulf , Schumann, Rhena and Jarvis, Suzanne P.(2009) 'Characterisation of Amyloid Nanostructures in the Natural Adhesive of Unicellular Subaerial Algae', The Journal of Adhesion, 85: 8, 465 — 483
To link to this Article: DOI: 10.1080/00218460902996366
URL: http://dx.doi.org/10.1080/00218460902996366

The Journal of Adhesion, 85:465–483, 2009

ISSN: 0021-8464 print/1545-5823 online
DOI: 10.1080/00218460902996366

Taylor & Francis
Taylor & Francis Group

Characterisation of Amyloid Nanostructures in the Natural Adhesive of Unicellular Subaerial Algae

Anika S. Mostaert[1,2], Cristiano Giordani[2], Rowena Crockett[3], Ulf Karsten[4], Rhena Schumann[4], and Suzanne P. Jarvis[2]
[1]School of Biology and Environmental Science, University College Dublin, Belfield, Dublin, Ireland
[2]Conway Institute of Biomolecular and Biomedical Research, University College Dublin, Belfield, Dublin, Ireland
[3]Swiss Federal Laboratories for Material Testing and Research, Duebendorf, Switzerland
[4]Institute of Biological Sciences, Applied Ecology, University of Rostock, Rostock, Germany

The composition and nanoscale mechanical characteristics of the adhesive from two species of subaerial green unicellular microalgae (Chlorophyta), Coccomyxa *sp. and* Glaphyrella trebouxiodes*, have been studied using Raman spectroscopy, chemical staining, and atomic force microscopy (AFM). Raman spectroscopy confirmed the adhesive proteins of both species to be predominantly in β-sheet conformations and composed of a number of hydrophobic amino acid residues. Chemical staining with Congo red and thioflavin-T dyes further confirmed the presence of amyloid-like structures. Probing the adhesives with AFM revealed highly ordered and repetitive mechanical responses indicative of highly ordered structures within the adhesive. The repetitive nature of the sawtooth response is typical of a "sacrificial bond" and "hidden length" mechanism, and what we propose is the result of mechanical manipulation of individual molecules within an intermolecular β-sheet that makes up the generic amyloid structure. The mechanical data show how amyloid provides cohesive strength to the adhesives, and this intrinsic mechanical property of an amyloid-based adhesive explains the ecological success of attachment of these subaerial microalgae on various surfaces in urban environments. It is unknown to what extent amyloid fibrils*

Received 9 October 2008; in final form 24 January 2009.

One of a Collection of papers honoring J. Herbert Waite, the recipient in February 2009 of *The Adhesion Society Award for Excellence in Adhesion Science, Sponsored by 3M*.

Address correspondence to Suzanne P. Jarvis or Anika S. Mostaert, Conway Institute of Biomolecular and Biomedical Research, University College Dublin, Belfield, Dublin 4, Ireland. E-mail: suzi.jarvis@ucd.ie or anika.mostaert@ucd.ie

occur in algal adhesives, but we postulate that the amyloid structure could provide a widespread mechanism for mechanical strength.

Keywords: Algae; Amyloid fibrils; Atomic force microscopy (AFM); Nanomechanics; Natural adhesives

INTRODUCTION

Subaerial green algae colonize the interface between a wide range of terrestrial surfaces and the atmosphere. Several hundred species have been identified [1], many of which form conspicuous biofilms on natural and artificial surfaces [2,3]. In urban areas, extensive growths on roof tiles, building facades, and concrete pathways constitute a biofouling problem [2]. Whether they actively corrode a surface material remains the subject of debate [4], but their discolouring patinas and incrustations, together with deterioration and accelerated weathering, have been described [4,5].

There is considerable evidence to suggest genetic adaptation to particular environmental factors in the terrestrial environment, such as heavy metals and herbicides [6]. Data for subaerial microalgae also show that, while optimal growth and photosynthesis occur under liquid culture conditions, these organisms can dry to inactivity then fully recover when rehydrated [7]. The underlying physiological and biochemical capabilities provide some explanation for the ecological success of algae in occupying large expanses of substrate in urban areas [8]. However, an important additional contribution to their ecological success is their ability to form a strong permanent adhesion to a wide range of substrates. In this article we explore the underlying mechanical mechanisms underpinning this permanent adhesion.

Successful establishment of subaerial algal spores or cells is dependent on local environmental conditions and the ability to attach rapidly and strongly to a surface. This is comparable with well-studied marine algae and is achieved by attachment *via* a two-stage process, initial and permanent adhesion, mediated by the secretion of extracellular polymeric substances (EPS) [9]. It is generally accepted that the EPS of algae have a diversity of structure, chemical composition, and function, but are predominantly polysaccharide-protein complexes, which strengthen over time through a curing process [9]. EPS is therefore considered to be a complex mixture of structural and functional proteins, glycoproteins, and proteoglycans arranged in a 3-D matrix structure.

While studies continue to attempt chemical characterization of algal EPS, mainly of diatoms [10,11], recent studies [12–15] have begun to explore the nanomechanical properties of algal adhesives using the atomic force microscope (AFM) [16]. The AFM is a particularly effective tool for measuring the adhesion of nanoscale volumes of material as it relies upon sensitive laser detection of the deflections of a small cantilever-mounted tip, in response to intermolecular forces between the tip and material of interest. This instrument allows measurement of the mechanical properties of single molecules such as DNA, modular proteins, and polysaccharides [17–20], and is able to directly probe mechanical properties of natural adhesives of living organisms *in situ* under ambient conditions and in liquid [21]. The underlying mechanisms of the strength of a natural adhesive may, thereby, be related to the structural properties of its constituent molecules, rather than to the biochemical identity of the specific molecules present [22].

In this paper, we investigate the nanoscale adhesive properties of two species of subaerial algae selected because of their observed strong attachment to anthropogenic surfaces in their urban habitats as well as to culture vessels in the laboratory. *Coccomyxa* sp. and *Glaphyrella trebouxiodes* are unicellular green microalgae (Chlorophyta, Trebouxiophyceae) that form extensive films on exposed roof tiles and building facades in European cities. We employed AFM to study the nanomechanical properties of natural adhesives of these algae, as well as Raman spectroscopy and chemical staining for *in situ* detection and characterization of protein structures.

EXPERIMENTAL

Algal Cultures

Two species of green subaerial algae (Chlorophyta, Trebouxiophyceae) were isolated from anthropogenic surfaces in urban habitats in Germany, and established as unialgal cultures (SAG culture collection, Göttingen, Germany). *Coccomyxa* sp. (SAG 2040, Fig. 1a) was collected in Unsleben, Bad Neustadt, Germany, where it grows as colonies of single cells forming conspicuous green films on exposed roof tiles (Fig. 1c). *Glaphyrella trebouxiodes* (SAG 2142, Fig. 1b) was originally isolated from a biofilm on a switchbox surface at a power supply station in Rostock, Germany (Fig. 1d), but is also found as extensive films on building facades in North East Germany (Fig. 1e). The cultures were maintained in a modified Bold's basal freshwater medium [23] at 10°C, 16:8 h light:dark cycle, 30–35 μmol photons m^{-2} s^{-1} illumination.

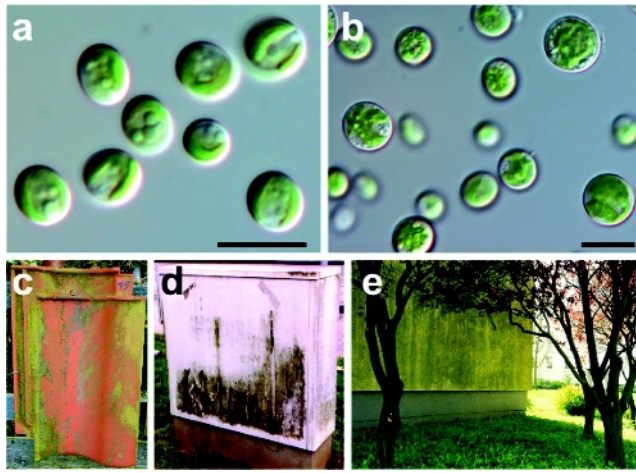

FIGURE 1 Light micrographs of (a) *Coccomyxa* sp. and (b) *Glaphyrella trebouxiodes* in culture. These images were made during log-phase growth using an Olympus BX51 light microscope with an SIS Colour View 12 camera. Scale bars = 10 μm. These algae grow as conspicuous green biofilms, often with other species, on artificial surfaces such as (c) *Coccomyxa* sp. shown here on a roof tile (tile size about 30 × 40 cm), and (d) *Glaphyrella trebouxiodes* on a plastic switchbox surface (switchbox height about 1 m), and (e) a building facade in North East Germany (Baltic Sea coast).

Attached Algae for Microscopy and Raman Spectrscopy

Approximately 10 mL of culture media with resuspended *Coccomyxa* sp. or *Glaphyrella trebouxiodes* was pipetted onto 22 mm glass coverslips in petri dishes. Cells were left to settle and attach directly onto the coverslips for 4 to 7 days before being washed in culture media to remove unattached cells. The coverslips were then used for light microscopy and SEM, or were glued onto glass slides immediately before investigation by AFM. Both species exhibited strong and rapid attachment to the coverslips making them ideal organisms for AFM where material must be immobilized. For Raman spectroscopy the same procedure for algal attachment was used, but glass slides were used instead of coverslips.

Scanning Electron Microscopy (SEM)

Algal cells attached onto glass coverslips as described above were fixed in 3% glutaraldehyde in 0.05 M phosphate buffer for 5 min, and

postfixed with 2% osmium tetroxide in 0.05 M phosphate buffer for 5 min. The coverslips with fixed cells were dehydrated in a graded acetone series and air dried before being gold sputtered and imaged with a field emission scanning electron microscope (Hitachi S-4300 FESEM, Hitachi Co. Ltd., Tokyo, Japan) at an accelerating voltage of 5 kV.

Atomic Force Microscopy (AFM)

AFM force measurements were made at room temperature (20°C) in pure water using an Asylum MFP-3D AFM (Asylum Research, Santa Barbara, CA, USA) mounted on top of an Olympus IX51 inverted optical microscope for visualizing and manually positioning regions to be probed. Force measurements were made at a rate of 0.3 to 0.5 Hz, using Si_3N_4 cantilevers (CSC38, MikroMasch, Tallinn, Estonia) with calibrated spring constants between 500 and 800 pN/nm. Force-extension curves were recorded at a rate of 1–2 μm/s, which is comparable with that used for stretching proteins [24,25]. Image processing and analysis of the force curves, including fitting each force peak with the worm-like chain model [26], were performed using IGOR PRO (Wavemetrics, Lake Oswego, OR, USA) data analysis software. All AFM measurements were made directly on three adhesive pads of both algal species, with at least 2000 force-extension curves taken for different regions of each adhesive pad.

Histochemical Staining: Congo Red

Algae attached to glass coverslips were treated directly with 0.5% Congo red (Sigma-Aldrich, Dublin, Ireland) in 50% ethanol [27] for 3 mins, before being washed with deionized water and mounted in glycerol gelatin (Sigma-Aldrich, Dublin, Ireland). Specimens were viewed immediately at 40× magnification with a Zeiss AxioCam 200 microscope (Carl Zeiss Ltd., Hertfordshire, UK) fitted with a polarizer and analyser for switching from bright field imaging to polarizing microscopy. Images were obtained using an AxioCam HR colour camera (Carl Zeiss Ltd, Hertfordshire, UK).

Histochemical Staining: Thioflavin-T

Confocal microscopy was used in order to detect the fluorophore thioflavin-T (Sigma-Aldrich, Dublin, Ireland) bound to amyloid structures [15,27] in the adhesives of both species of algae. A Zeiss confocal Meta system (LSM 510, Carl Zeiss Ltd., Hertfordshire, UK) was used

to allow separation of multiple fluorophore based on their emission spectra. The algal autofluorescence due to the presence of chlorophyll was evident at 680 nm, as determined by exciting an unstained control sample at 488 nm and collecting the emission between 505 and 700 nm. Emission of thiofavin-T binding to a control sample of amyloid fibrils grown from a synthesized amyloid β-protein$_{25-35}$ (H-1192, Bachem, Merseyside, UK) was determined using the same procedure as described previously [15]. Sample binding by thioflavin-T was detected by directly staining algae attached to coverslips with 10 μM aqueous thioflavin-T for 5 mins before being washed in pure water. Thioflavin-T stained algae were again excited at 488 nm and emission collected between 505 and 700 nm. Using the two control emission spectra, it was possible to separate the alga's autofluorescence from the amyloid in the adhesive region stained with thioflavin-T.

Raman Spectroscopy

Raman spectra were recorded on different areas of adhesive surrounding cells from both species attached to glass slides. The spectrum with the best signal-to-noise ratio and highest intensity was selected for further analysis. Spectra were collected using a Renishaw MicroRaman (Renishaw, Gloucestershire, UK) with a diode laser (780 nm) and a magnification of 50×. The power measured at the sample was 2.8 mW. Contamination and artifacts were identified by measuring spectra in different areas and comparing the intensities of the peaks. In this way, part of the intensity of the peak at 1047 cm^{-1} in the spectrum for *Glaphyrella trebouxiodes* (Fig. 6) is considered to be an artifact.

RESULTS AND DISCUSSION

Scanning electron microscopy of *Coccomyxa* sp. and *Glaphyrella trebouxiodes* reveals the EPS layer covering the surface of each cell, and a differentiated region of EPS secreted beneath the cell forming a discrete adhesive pad functioning for permanent strong adhesion (Fig. 2). For both algal species, it was necessary to dislodge cells from the adhesive pads to gain access to the cell adhesive interface for probing with the AFM tip. This was achieved by either scanning the AFM tip across a cell (Fig. 3a), or, more often, by scraping the surface with the edge of a glass slide because the cells were so strongly attached (Fig. 3b). This allowed force measurements to be made directly from different regions of the freshly exposed adhesive. In the case of Raman spectroscopy, it was possible to collect spectra directly from regions of adhesive surrounding the cells as dehydration allowed more

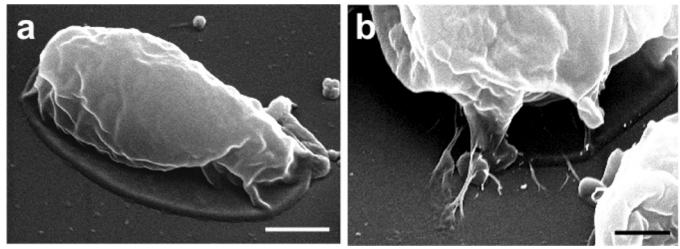

FIGURE 2 SEM images of algal cells attached to glass coverslips. After 4 days, the EPS layer covering the surface of each cell and differentiated EPS forming the adhesive pads beneath the cells can be seen for both (a) *Coccomyxa* sp. and (b) *Glaphyrella trebouxiodes*. Scale bars = 1 μm.

accessibility. This is not dissimilar to the SEM image (Fig. 2a) of *Coccomyxa* sp. where preparation for SEM resulted in some dehydration of the material that is normally hydrated in its native state.

We used AFM to measure the tensile mechanical properties of the adhesives of both species of algae *in situ*, and under ambient conditions, in order to elucidate any underlying molecular structural properties that may influence the bulk mechanical properties of the adhesive. To do this, the tip of the AFM cantilever was positioned on numerous regions to allow force-extension curves to be taken.

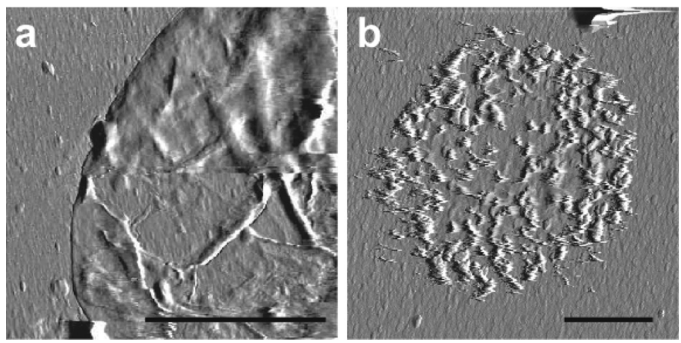

FIGURE 3 AFM images of adhesive pads of (a) *Coccomyxa* sp. and (b) *Glaphyrella trebouxiodes* attached to the surface of glass slides. In the case of (a) *Coccomyxa* sp. the algal cell was physically dislodged from the adhesive pad by the AFM tip and for (b) *Glaphyrella trebouxiodes*, the cell had been scraped from the surface to reveal the persistent adhesive pad underneath. Force measurements could then be made from different regions of the freshly exposed adhesive. AFM force measurements were made on pad surfaces within 1 week following cell settlement. Scale bars = 2 μm.

The resulting force-extension curves predominantly (72%) produced random unbinding events, as we have observed previously from the adhesive holdfast of the green multicellular macroalga, *Prasiola linearis* [15,28]. Such curves are not surprising from a complex biocomposite typical of an algal EPS; however, as also observed for *P. linearis*, curves regularly (here 18%) showed highly ordered sawtooth patterns (Fig. 4). The sawtooth peaks were remarkably regularly spaced with a separation of approximately 36 nm [38.3 ± 6.1 nm ($n = 108$) for *Glaphyrella trebouxiodes* and 34.0 ± 5.6 nm ($n = 411$) for *Coccomyxa* sp.], indicating an underlying structurally repetitive material. Sawtooth mechanical responses, such as these, are associated with

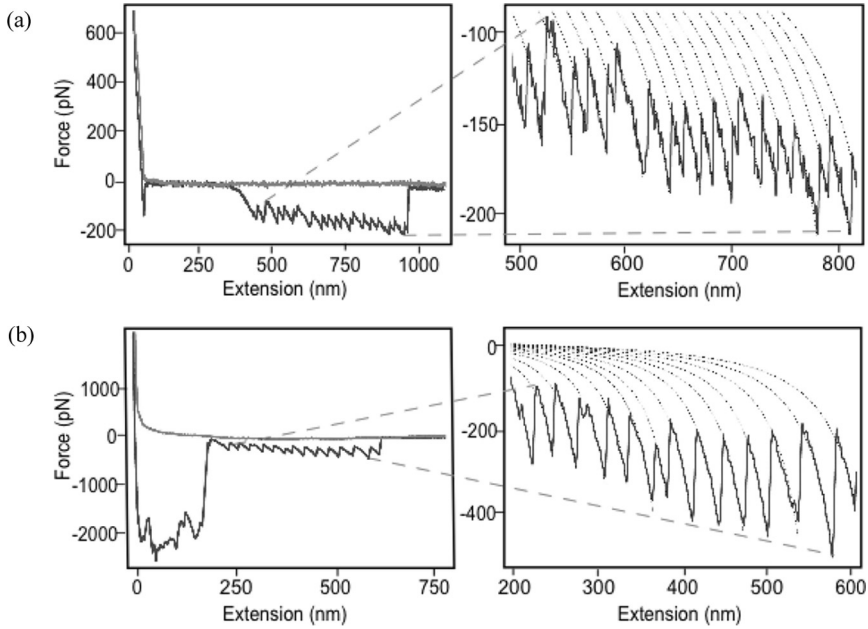

FIGURE 4 Representative AFM force-extension curves showing sawtooth structures. Both the approach (smooth curve) and retraction (sawtooth curve) force traces are shown for curves on the left. Expansions of the sawtooth region of each force-extension curve are also shown on the right fitted to the worm-like chain model (dotted lines). This specific curve for (a) *Coccomyxa* sp. has a mean persistence length of 0.40 nm and a mean contour length of 32.8 nm. For the representative curve of (b) *Glaphyrella trebouxiodes*, the mean persistence length was 0.36 for the 13 peaks, with a mean contour length of 31.4 nm. Sawtooth structures such as these occurred in localized regions of the EPS adhesive.

materials exhibiting high mechanical strength due to the large amount of energy required to break sequential units of "sacrifical bonds" and extend the exposed "hidden length" [22]. An additional mechanical benefit of this structural biopolymer was evident as the sawtooth pattern was reproducible when successive curves were taken at the same location, indicating a strong ability of the material to reform or re-assemble at the same location (Fig. 5).

Further quantification of the mechanical response was performed by fitting the biopolymer using a worm-like chain fit for the elastic part of the tensile response. This revealed a mean persistence length of 0.44 ± 0.08 nm for *Coccomyxa* sp. (Fig. 4a), and 0.38 ± 0.07 nm for *Glaphyrella trebouxiodes* (Fig. 4b). In both cases, the persistence length is consistent for the size of an amino acid in a polypeptide chain.

To date, two alternative explanations have been proposed for sawtooth mechanical responses from natural adhesives. Wetherbee and

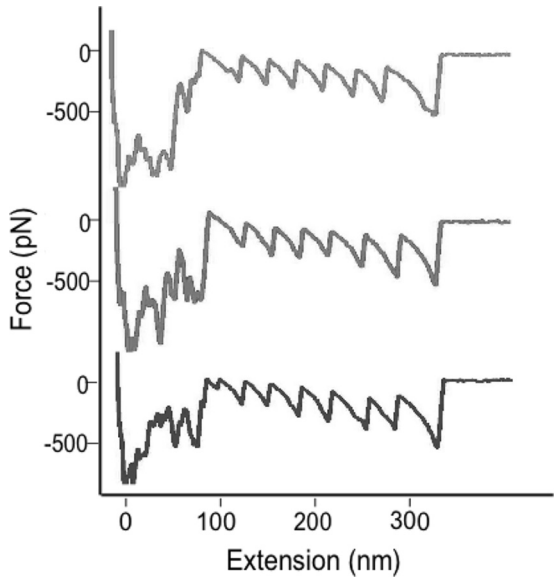

FIGURE 5 Sequential AFM force-extension curves suggesting that the reforming of intermolecular ß-sheets has occurred under the tip. These successive force curves from the same position on the adhesive pad of *Glaphyrella trebouxiodes* are very similar and superimposable in the sawtooth region although they all exhibit different non-specific adhesion as would be expected for three different tip-sample contacts.

co-workers have proposed the presence of large (>220 kDa), single, structurally modular proteins arranged into perfectly aligned parallel polymers (termed "adhesive nanofibers") that function as a cohesive unit, for diatom adhesives with different functions. This includes the permanent adhesive pad secreted by the centric diatom *Toxarium undulatum* [11,12,14] and the temporary adhesive EPS secreted by the motile, pennate diatom *Phaeodactylum tricornutum* [13]. To date there has been no identification of any protein from the family of structurally homologous proteins that would need to exist in order to explain the observed sawtooth responses of different dimensions found from an increasing number of different natural adhesives. Our preferred explanation is that the response is due to pulling on a functional form of amyloid in the adhesive [15,28,29], whereby sawtooths indicate the successive unravelling of linked small proteins from the intermolecular β-sheets making up the amyloid fibril structure. This is based on mechanical arguments linking a number of unusual measured mechanical responses to the generic amyloid core structure that cannot be explained by a large single molecule [28]. Our preferred explanation is further supported by other reports of functional amyloid in natural materials as described in more detail below. Central to our argument is that amyloid can be formed from a broad range of polypeptides of widely varying size and composition, thus, unlike the alternative hypothesis, there is no need to invoke any structural link between the native proteins themselves, making additional discoveries of regular mechanical responses from the adhesives of different organisms less surprising.

The structure of amyloid can be defined as orderly repeats of protein molecules arranged as a fibril of indefinite length in a cross-beta structure, in which intramolecular β-stands run perpendicular to the fibril axis and intermolecular β-sheets run parallel to the fibril axis [30]. Amyloid is associated with debilitating human diseases such as Alzheimer's and Parkinson's [31], and many other "misfolding" disorders such as type II diabetes, kuru, and Creutzfeldt-Jacob disease. The proteins involved in these diseases have unique and characteristic native folds, but the fibrils found in the disease states remarkably have structurally similar characteristics [32]. In recent years, striking evidence has accumulated to suggest the ability of proteins to self assemble into fibrils with the same overall structure is not a peculiarity of these disease-related proteins but rather, that essentially all proteins can form such structures under appropriate conditions [33]. This suggestion implies amyloid is a generic property of the polypeptide chain [33]. Consistent with this hypothesis are the recent discoveries of non-pathological amyloid

TABLE 1 Functional, Non-Pathological Amyloid in Different Organisms

Organism, species and amyloid location	Protein and explanation of function	Key references
Pacific Hagfish slime, *Eptatretus stoutii*	Slime of mucus and amyloid-like protein threads used as a defence mechanism, whereby gills of predators may become clogged. Amyloid content presumably provides mechanical strength to the slime.	34,35
Human melanoma cells, *Homo sapiens*	Pmel17 amyloid fibrils provide a template for scaffolding and sequestration during melanin synthesis.	36
Chorion in fish and insect egg shells, e.g., silkmoth, *Bombyx mori*	Chorion proteins self-assemble into spherulites, which convert to amyloid fibrils upon egg shell maturation forming a protective coating for the oocyte and embryo.	37,38
Sea slugs synapses, *Aplysia californica*	Engineered expression of the *Aplysia* synapse protein CPEB in yeast yields prion-like aggregates, hence prion-like states of CPEB might affect long-term synaptic contact.	39
Hydrophobins coatings of many fungi, e.g., *Neurospora crassa, Aspergillus nidulans*	Hydrophobins provide resistance to desiccation stress, as well as modulation of adhesion and surface tension.	40–42
Bacterial biolfilm (curli), *Escherichia coli*, *Salmonella*, and many others	Curli fibers in extruded biofilm promote host invasion, surface colonization, and provide cohesive and adhesive strength to the biofilm.	29,43,44
Bacterial chaplins, *Streptomyces coelicolor*	Secreted hydrophobic chaplins form aerial hyphae with a coating that modulates water surface tension.	41,45
Amyloid-based prions in fungi, e.g., yeast (*Saccharomyces cerevisiae*) and *Podospora anserine*	Aggregation of Sup35p in yeast can actively confer phenotype, and may provide some stress protection. Ure2p regulates nitrogen catabolism in yeast, and Het-s regulates heterokaryon formation.	46–52
Macroalgal adhesive, *Prasiola linearis* (Chlorophyta)	Amyloid discovered in this permanent natural adhesive and believed to be the mechanism for cohesive and adhesive strength.	15

(*Continued*)

TABLE 1 Continued

Organism, species and amyloid location	Protein and explanation of function	Key references
Spider silk spidroins, *Nephila edulis, N. clavipes, Araneus diadematus*	Spiders form insoluble filaments of fibroin protein, and amyloid-like cross-ß structure develops in a region of reduced pH downstream from the initial extrusion site. Provides strength and elasticity to silk threads.	53–55
Marine parasite adhesive, *Entobdella soleae* (Monogenean)	Amyloid identified in the extruded adhesive of the fish skin parasite believed to provide both cohesive and adhesive strength to this temporary marine adhesive.	29
Barnacle cement, *Semibalanus balanoides*	Similarities are identified between barnacle cement and amyloid plaques, with regards to the rich ß-sheet structure and molecular mechanism of forming an insoluble proteinaceous multimer.	56

fibrils from different organisms, some of which have already been identified to have important physiological roles (see Table 1 for summary). The lack of dependence of the amyloid generic structure on amino acid sequence provides an explanation for the apparent widespread occurrence of amyloid in natural adhesives from a broad range of organisms (Table 1, and references therein).

With the amyloid explanation for the sawtooth response, each jump corresponds to the instantaneous unfolding of a protein within an intermolecular β-sheet and each elastic stretch corresponds to the extension of the hidden length exposed within the unfolded protein chain. Thus, with this model the constituent proteins are expected to be somewhat larger than 90 amino acids (calculated from the hidden length of 36 nm divided by the size of a single amino acid of approximately 0.4 nm). This calculation slightly underestimates the size of the protein as the folded length is not known and the total length is given by adding together the measured hidden length and the folded length.

It should be noted that there is no proof that mechanical responses such as these represent signatures or fingerprints of a particular molecular structure and, thus, AFM cannot be used as a means of identifying the presence of amyloid. To support our proposed model

we utilized the additional techniques of Raman spectroscopy and histochemical staining with the amyloid-binding dyes Congo red and thioflavin-T.

We can identify the same peaks in the Raman spectra of both algal species (Fig. 6). Band assignments for the peaks were determined and these are presented in Table 2. The amide III band is typical for a β-sheet structure with peaks at 1224 and 1260 cm^{-1} [57,58,59]. The peak at 1606 cm^{-1} is in a region that is normally associated with phenylalanine, tryptophan, or tyrosine; however, the other Raman peaks associated with these amino acids were not present in intensities that would justify such an assignment. If a peak of the intensity

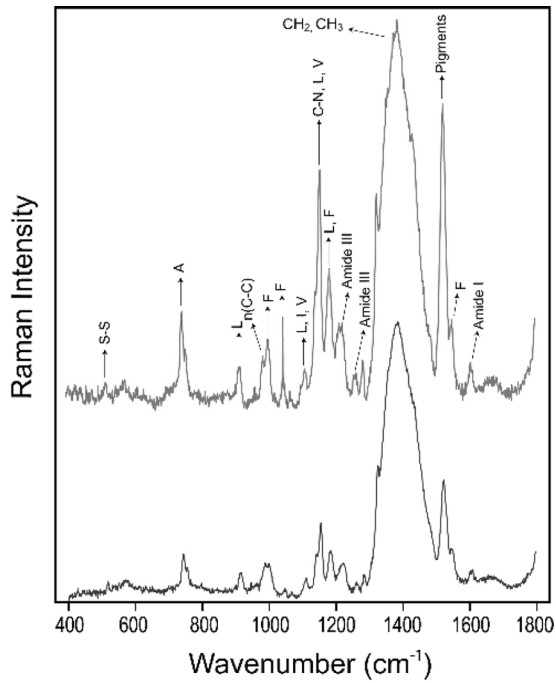

FIGURE 6 Typical Raman spectra observed for regions of the adhesive of both *Glaphyrella trebouxiodes* (upper spectrum) and *Coccomyxa* sp. (lower spectrum). The amide III band was typical for a β-sheet structure with maxima at 1224 and 1260 cm^{-1} (upper) and 1223 and 1262 cm^{-1} (lower). The strong peak at 1525 (upper) and 1523 cm^{-1} (lower) was assigned to carotenoid pigments. The Raman spectrum contains a low value for the amide I peak at 1606 cm^{-1} (both spectra). Amino acids contained in the algal adhesive are indicated by the arrows using the one-letter standard amino acid abbreviation.

TABLE 2 Assignment of Bands in Raman Spectrum for *Glaphyrella Trebouxiodes* and *Coccomyxa* sp. (Wavenumbers in Parentheses are Those for *Coccomyxa* sp.)

Wavenumber [cm^{-1}]	Band assignment(s)	Key references
520 (518)	S-S stretching	57
746 (744)	Ala	58
920 (918)	Leu	59
988 (988)	n (C-C)	57
1002, 1047 (1000, 1047)	Phe	57
1113 (1112)	Leu, Ile, Val	58,59
1157 (1155)	C-N, Leu, Val	58,59
1186 (1185)	Leu, Phe	57–59
1224, 1260 (1223, 1262)	Amide III	57–60
1327 (1326)	δ (CH)	57
1388–1450, (1386–1450)	δ (CH_2)(CH_3)	57
1525 (1523)	Pigments	60
1551 (1547)	Phe	57
1606 (1606)	Amide I (ß-sheet)	61,30

of that at 1606 cm^{-1} resulted from the vibration of bonds in these amino acids then the spectrum would be dominated by a peak at 1002 cm^{-1}. As this is not the case, the peak at 1606 cm^{-1} was attributed to the (π,0) mode of the amide bond. Unusually low values for an amide I band are thought to be due to exceptionally strong hydrogen bonding [58]. The unusually low value for an amide I band at 1606 cm^{-1} may be typical of an amyloid structure, due to the strong intermolecular networks of hydrogen bonding stabilizing the stacks of β-strands [61,30]. The strong peak at 1525 cm^{-1} is indicative of carotenoid pigments [60], which are typically present in the green algae. The peak at 520 cm^{-1} is assigned to S-S bonds [57]. It is interesting to note that all the residues identified in the spectra are hydrophobic. Peaks at 1002, 1047, 1186, and 1551 cm^{-1} were assigned to phenylalanine (F), the peak at 746 cm^{-1} to alanine (A), and peaks at 920, 1113 [overlapped with valine (V) and isoleucine (I)], 1157 (overlapped with V), and 1186 cm^{-1} to leucine (L). The presence and location of amide I and III, and the detected residues being hydrophobic, are consistent with a generic amyloid structure with a strongly hydrophobic core.

Direct binding of thioflavin-T in the adhesive region of the cells was detected with confocal microscopy (Fig. 7). This dye exhibits fluorescence upon binding to amyloid fibrils [27] (Fig. 8). A faint positive signal was also visible from the cells themselves, which may be due to the thioflavin-T binding to intracellular DNA (Fig. 7a). The cellular region could be distinguished from the adhesive region

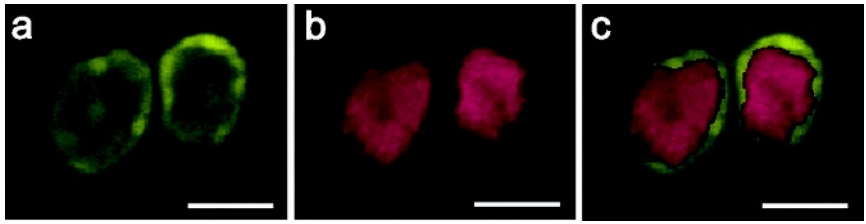

FIGURE 7 Direct binding of thioflavin-T to ß-sheet structures within the adhesive of *Glaphyrella trebouxiodes*. Algae attached to glass slides were stained directly with thioflavin-T. Zeiss confocal Meta microscopy allows separation of the emission of the (a) thioflavin-T bound ß-sheet structures and (b) the algal autofluorescence at 575 and 682 nm, respectively. An overlay between (a) and (b) is shown in (c). The adhesive around the individual algal cells produced a positive signal for thioflavin-T. Scale bars = 5 μm.

(Fig. 7c) by overlaying the autofluorescence image of the algae (Fig. 7b) with the larger thioflavin-T stained region (Fig. 7a). As DNA is not found in the EPS, the positive thioflavin-T signal in the region outside the cells (Fig. 7c) was taken as an indication of extracellular amyloid fibrils in the adhesive matrix.

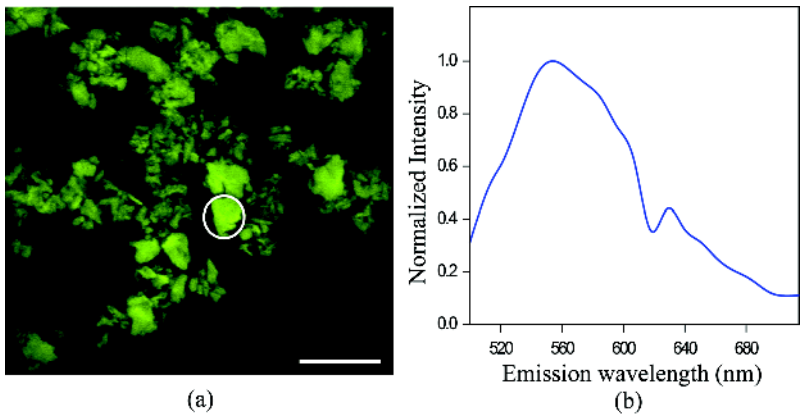

FIGURE 8 Binding of thioflavin-T to a control sample of amyloid ß-protein. (a) Confocal microscope image of amyloid ß-protein stained with the fluorophore thioflavin-T. Scale bar = 50 μm. (b) Confocal emission spectrum of thioflavin-T bound amyloid β-protein fibrils from the region circled in (a) after excitation at 488 nm.

In the case of Congo red staining, the extremely small amount of adhesive produced by individual algal cells made amyloid detection by this dye impractical for cells *in situ*. Typically, an amyloid sample of 10 μm thickness is required to obtain a clear green-gold birefringence under cross-polarized light with this staining technique. When the cells and adhesive EPS were mechanically gathered into an isolated region, enough biomass of material allowed staining and clear birefringence in the adhesive EPS to be observed (Fig. 9).

All the above methods provide support for the presence of amyloid in the material. Conclusive proof is only really possible with X-ray fibril diffraction studies; however, the application of this technique to *ex vivo* samples is extremely challenging [62] and will require further developments in sample preparation before this can be meaningfully applied to natural adhesives presented here.

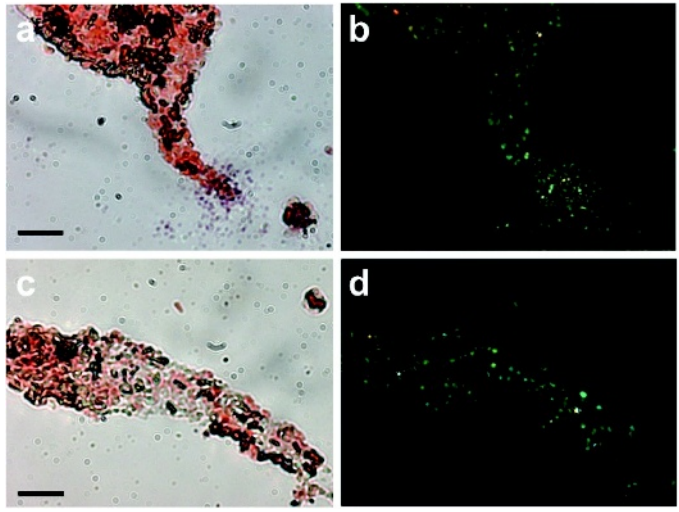

FIGURE 9 Evidence of amyloid in algal adhesives indicated by Congo red staining. Images on the left are bright field and those on the right are taken with cross-polarizers. Images (a) and (b) are from *Coccomyxa* sp., and (c) and (d) are *Glaphyrella trebouxiodes*. The algal cells and adhesive EPS were scraped into an isolated region for staining. Bright field images show binding of the amyloid-selective dye, and the same regions show green-gold birefringence under cross-polarized light characteristic of amyloid structures. Scale bars = 100 μm.

CONCLUSION

In conclusion, we have established that the natural adhesives of two representative species of subaerial, unicellular microalgae exhibit the same underlying nanoscale repetitive sawtooth response to a tensile force as those measured for adhesives from multicellular subaerial algae [15], diatoms [12,13], a parasitic flatworm [29], and the bacterial amyloid-based biofilm, curli [29]. A large body of literature exists describing the structure and performance of natural adhesives, but often with an emphasis on the diversity of biological adhesives [22,63], rather than highlighting any shared underlying mechanisms. Yet to understand the fundamental processes leading to adhesion, we must first focus on the phenomena that many systems appear to have in common. Our proposed model is that the ultrastructures in the adhesive are mechanically functional amyloid fibrils composed of, as yet unidentified, small proteins. If correct, this mechanism would provide a generic link between aqueous and terrestrial adhesives, and permanent and temporary adhesives, occurring in numerous organisms of phylogenetically different phyla including invertebrates, algae, and bacteria.

ACKNOWLEDGMENT

We thank Professor Thomas Friedl, University of Göttingen, Germany, for supplying the algal isolates for the cultures used in these experiments. We are very grateful to Manuela Görs, University of Rostock, Germany, for assistance with cultures prepared for the Raman spectroscopy and the light micrographs. This work was funded by Science Foundation Ireland (07/IN1/B931), and in part by the Deutsche Forschungsgemeinschaft (Ka 899-13/1).

REFERENCES

[1] Ettl, H. and Gärtner, G., *Syllabus der Boden-, Luft-und Flechtenalgen*, (Gustav Fischer Verlag, Stuttgart, Germany, 1995), p. 721.
[2] Rindi, F. and Guiry, M. D., *Crytogamie Algol.* **24**, 245–267 (2003).
[3] Eggert, A., Häubner, N., Klausch, S., Karsten, U., and Schumann, R., *Biofouling* **22**, 79–90 (2006).
[4] Ortega-Calvo, J. J., Arino, X., Hernandez-Marine, M., and Saiz-Jimenez, C., *Sci. Tot. Environ.* **167**, 329–341 (1995).
[5] Gaylarde, C. C. and Morton, L. H. G., *Biolfouling* **14**, 59–74 (1999).
[6] García-Meza, J. V., Barranguet, C., and Admiraal, W., *Environ. Toxicol. Chem.* **24**, 573–581 (2005).
[7] Häubner, N., Schumann, R., and Karsten, U., *Microb. Ecol.* **51**, 285–293 (2006).
[8] Karsten, U., Schumann, R., and Mostaert, A., in *Cellular Origins, Life in Extreme Habitats and Astrobiology. Extremophilic and Enigmatic Algae and*

Non-Photosynthetic Protists, J. Seckbach (Ed.) (Springer, Dordrecht, The Netherlands, 2007), pp. 585–597.
[9] Fletcher, R. L. and Callow, M. E., *Br. Phycol. J.* **27**, 303–329 (1992).
[10] Stal, L. J., *Geomicro. J.* **20**, 463–478 (2003).
[11] Chiovitti, A., Heraud, P., Dugdale, T. M., Hodson, O. M., Curtain, R. C. A., Dagastine, R. R., Wood, B. R., and Wetherbee, R., *Soft Matter* **4**, 811–820 (2008).
[12] Dugdale, T. M., Dagastine, R., Chiovitti, A., Mulvaney, P., and Wetherbee, R. *Biophys. J.* **89**, 4252–4260 (2005).
[13] Dugdale, T. M., Dagastine, R., Chiovitti, A., and Wetherbee, R., *Biophys. J.* **90**, 2987–2993 (2006).
[14] Dugdale, T. M., Willis, A., and Wetherbee, R., *Biophys. J.* **90**, L58–L60 (2006).
[15] Mostaert, A. S., Higgins, M. J., Fukuma, T., Rindi, F., and Jarvis, S. P., *J. Biol. Phys.* **32**, 393–401 (2006).
[16] Binnig, G., Quate, C. F., and Gerber, C., *Phys. Rev. Lett.* **56**, 930–933 (1986).
[17] Engel, A., Gaub, H. E., and Müller, D. J., *Curr. Biol.* **9**, 133–136 (1999).
[18] Engel, A. and Müller, D. J., *Nat. Struct. Biol.* **7**, 715–718 (2000).
[19] Fisher, T. E., Marszalek, P. E., and Fernandez, J. M., *Nat. Struct. Biol.* **7**, 719–723 (2000).
[20] Clausen-Schaumann, H., Seiz, M., Krautbauer, R., and Gaub, H. E., *Curr. Opin. Chem. Biol.* **4**, 524–530 (2000).
[21] Dufrêne, Y. F., *Nat. Rev. Microbiol.* **2**, 451–460 (2004).
[22] Smith, B. L., Schäffer, T. E., Viani, M., Thompson, J. B., Frederick, N. A., Kindt, J., Belcher, A., Stucky, G. D., Morse, D. E., and Hansma, P. K., *Nature* **399**, 761–763 (1999).
[23] Guiry, M. D. and Cunningham, E. M., *Phycologia* **23**, 357–367 (1984).
[24] Rief, M., Gautel, M., Oesterhelt, F., Fernandez, J. M., and Gaub, H. E., *Science* **276**, 1109–1112 (1997).
[25] Best, R. B. and Clark, J., *Chem. Commun.* **18**, 183–192 (2002).
[26] Bustamante, C., Marko, J. F., Siggia, E. D., and Smith, S., *Science* **265**, 1599–1600 (1994).
[27] Vowles, G. H. and Francis, R. J., in *Theory and Practice of Histological Techniques*, J. D. Bancroft and M. Gamble (Eds.) (Churchill Livingstone, London, 2002), pp. 303–324.
[28] Mostaert, A. S. and Jarvis, S. P., *Nanotechnology* **18**, 044010 (2007).
[29] Mostaert, A. S., Crockett, R., Kearn, G., Cherny, I., Gazit, E., Serpell, L. C., and Jarvis, S. P. *J. Adhesion*, accepted.
[30] Sunde, M. and Blake, C., *Adv. Protein Chem.* **50**, 123–159 (1997).
[31] Dobson, C. M., *Nature* **426**, 884–890 (2003).
[32] Sunde, M., Serpell, L. C., Bartlam, M., Fraser, P. E., Pepys, M. B., and Blake, C. C., *J. Mol. Biol.* **273**, 729–739 (1997).
[33] Chiti, F., Webster, P., Taddei, N., Clark, A., Stefani, M., Ramponi, G., and Dobson, C. M., *Proc. Natl. Acad. Sci. USA* **96**, 3590–3594 (1999).
[34] Fudge, D. S., Gardner, K. H., Forsyth, V. T., Riekel, C., and Gosline, J. M., *Biophys. J.* **85**, 2015–2027 (2003).
[35] Fudge, D. S., Levy, N., Chiu, S., and Gosline, J. M., *J. Exp. Biol.* **208**, 4613–4625 (2005).
[36] Fowler, D. M., Koulov, A. V., Alory-Jost, C., Marks, M. S., Balch, W. E., and Kelly, J. W., *PLoS Biol.* **4**, e6 (2005).
[37] Iconomidou, V. A., Vriend, G., and Hamodrakas, S. J., *FEBS Letters* **479**, 141–145 (2000).

[38] Hamodrakas, S. J., Hoenger, A., and Iconomidou, V. A., *J. Struct. Biol.* **145**, 226–235 (2004).
[39] Si, K., Lindquist, S. L., and Kandel, E. R., *Cell* **115**, 879–891 (2003).
[40] Mackay, J. P., Matthews, J. M., Winefield, R. D., Mackay, L.G., Haverkamp, R. G., and Templeton, M. D., *Structure* **9**, 83–91 (2001).
[41] Gebbink, M. F., Claessen, D., Bouma, B., Dijkhuizen, L., and Wosten, H. A., *Nat. Rev. Microbiol.* **3**, 333–341 (2005).
[42] Kwan, A. H. Y., Winefield, R. D., Sunde, M., Matthews, J. M., Haverkamp, R. G., Templeton, M. D., and Mackay, J. P., *Proc. Natl. Acad. Sci. USA* **103**, 3621–3626 (2006).
[43] Chapman, M. R., Robinson, L. S., Pinkner, J. S., Roth, R., Heuser, J., Hammer, M., Normack, S., and Hultgren, S. J., *Science* **295**, 851–855 (2002).
[44] Cherny, I., Rockah, L., Levy-Nissenbaum, O., Gophna, U., Ron, E. Z., and Gazit, E., *J. Mol. Biol.* **352**, 245–252 (2005).
[45] Claessen, D., Rink, R., de Jong, W., Siebring, J., de Vreugd, P., Boersma, F. G., Dijkhuizen, L., and Wosten, H. A., *Genes Dev.* **17**, 1714–1726 (2003).
[46] King, C.-Y., Tittmann, P., Gross, H., Gebert, R., Aebi, M., and Wuthrich, K., *Proc. Natl. Acad. Sci. USA* **94**, 6618–6622 (1997).
[47] True, H. L. and Lindquist, S. L., *Nature* **407**, 477–483 (2000).
[48] Dos Reis, S., Coulary-Salin, B., Forge, V., Lascu, I., Bégueret, J., and Saupe, S. J., *J. Biol. Chem.* **277**, 5703–5706 (2002).
[49] Shorter, J. and Lindquist, S. L., *Science* **304**, 1793–1797 (2004).
[50] True, H. L., Berlin, I., and Lindquist, S. L., *Nature* **431**, 184–187 (2004).
[51] Baxa, U., Cheng, N., Winkler, D. C., Chiu, T. K., Davies, D. R., Sharma, D., Inouye, H., Kirschner, D. A., Wickner, R. B., and Steven, A. C., *J. Struct. Biol.* **150**, 170–179 (2005).
[52] Ritter, C., Maddelein, M. L., Siemer, A. B., Lührs, T., Ernst, M., Meier, B. H., Saupe, S. J., and Riek, R., *Nature* **435**, 844–848 (2005).
[53] Kenney, J. M., Knight, D., Wise, M. J., and Vollrath, F., *Eur. J. Biochem.* **269**, 4159 (2002).
[54] Huemmerich, D., Helsen, C., Quedzuweit, S., Oschmann, R., Rudolph, R., and Scheibel, T., *Biochemistry* **43**, 13604 (2004).
[55] Slotta, U., Hess, S., Spieß, Stromer, T., Serpell, L., and Scheibel, T., *Macromol. Biosci.* **7**, 183–188 (2007).
[56] Kamino, K., Inoue, K., Maruyama, T., Takamatsu, N., Harayama, S., and Shizuri, Y., *J. Biol. Chem.* **275**, 27360–27365 (2000).
[57] Chou, I. H., Benford, M., Beier, H. T., Coté, G. L., Wang, M., Jing, N., Kameoka, J., and Good, T. A., *Nano Lett.* **8**, 1729–1735 (2008).
[58] Dong, J., Atwood, C. S., Anderson, V. E., Siedlak, S. L., Smith, M. A., Perry, G., and Carey, P. R., *Biochemistry* **42**, 2768–2773 (2003).
[59] Overman, S. A. and Thomas, G. J., *Biochemistry* **38**, 4018–4027 (1999).
[60] Naumann, D., in *Infrared and Raman Spectroscopy of Biological Materials*, H. U. Gremlich and B. Yan (Eds.) (Marcel Dekker, New York, 2001), pp. 323–377.
[61] Barth, A. and Zscherp, C., *Q. Rev. Biophys.* **35**, 369–430 (2002).
[62] Serpell, L. C., Benson, M., Liepnieks, J. J., and Fraser, P. E., *Amyloid* **14**, 199–203 (2007).
[63] Smith, A. M. and Callow, J. A., *Biological Adhesives*, (Springer, Heidelberg, Germany, 2006), p. 284.